Advances in Aircraft and Spacecraft Science, *Vol. 7, No. 3 (2020) 229-249*
DOI: https://doi.org/10.12989/aas.2020.7.3.229

Influence of the Mars atmosphere model on aerodynamics of an entry capsule: Part II

Gennaro Zuppardi*

Department of Industrial Engineering – Aerospace Division, University of Naples "Federico II", Piazzale Tecchio, 80 – 80125 Naples, Italy

(Received March 7, 2019, Revised December 10, 2019, Accepted December 30, 2019)

Abstract. This paper is the logical follow-up of four papers by the author on the subject "aerodynamics in Mars atmosphere". The aim of the papers was to evaluate the influence of two Mars atmosphere models (NASA Glenn and GRAM-2001) on aerodynamics of a capsule (Pathfinder) entering the Mars atmosphere and also to verify the feasibility of evaluating experimentally the ambient density and the ambient pressure by means of the methods by McLaughlin and Cassanto respectively, therefore to correct the values provided by the models. The study was carried out computationally by means of: i) a code integrating the equations of dynamics of an entry capsule for the computation of the trajectories, ii) two Direct Simulation Monte Carlo (DSMC) codes for the solution of the 2-D, axial-symmetric and 3-D flow fields around the capsule in the altitude interval 50-100 km. The computations verified that the entry trajectories of Pathfinder from the two models, in terms of the Mach, Reynolds and Knudsen numbers, were very different. The aim of the present paper is to continue this study, considering other aerodynamic problems and then to provide a contribution to a long series of papers on the subject "aerodynamics in Mars atmosphere". More specifically, the present paper evaluated and quantified the effects from the two models of: i) chemical reactions on aerodynamic quantities in the shock layer, ii) surface temperature, therefore of the contribution of the re-emitted molecules, on local (pressure, skin friction, etc.) and on global (drag) quantities, iii) surface recombination reactions (catalyticity) on heat flux. The results verified that the models heavily influence the flow field (as per the shock wave structure) but, apart from the surface recombination reactions, the effects of the different conditions on aerodynamics of the capsule are negligible for both models and confirmed what already found in the previous paper that, because of the higher values of density from the NASA Glenn model, the effects on aerodynamics of a entry capsule are stronger than those computed by the GRAM-2001 model.

Keywords: Mars atmosphere models; Mars Pathfinder capsule; entry trajectory; effects of surface temperature; effects of chemistry; effects of surface catalyticity; Direct Simulation Monte Carlo method

1. Introduction

This paper is the logical follow-up of four papers by the author (Zuppardi 2018a, b, 2019a, b) where: i) the influence of the atmosphere model was evaluated on aerodynamics of an axial-symmetric body, representing the nose of an aero-space-plane, entering the Mars and the Earth atmosphere (2018a), ii) the Shock Wave-Boundary Layer Interaction (SWBLI) and the Shock Wave-Shock Wave Interaction (SWSWI) in Mars atmosphere were studied (2018b), iii) the

*Corresponding author, Lecturer, E-mail: zuppardi@unina.it

http://www.techno-press.org/?journal=aas&subpage=7 ISSN: 2287-528X (Print), 2287-5271 (Online)

influence of two Mars atmosphere models was evaluated on 2-D (2019a) and 3-D (2019b) aerodynamics of the Mars Pathfinder capsule (Braun and Manning 2006).

The entry trajectories were computed by a code integrating the equations of dynamics of a non lifting body in free entry, i.e., with no parachute and with no thrusters (Zuppardi and Savino 2015). Since the computations were carried out at altitudes higher than 50 km, where a flow field is in transitional regime, the use of DSMC codes for the solution of the 2-D, axial-symmetric flow field (DS2V-4.5 64 bits (Bird 2012)) and of the 3-D flow field (DS3V (Bird 2005a)) has been mandatory.

More specifically the aim of:

1) the first paper (2018a) was to compare the effects of chemistry of the Earth and Mars atmosphere on heat flux of an entry body. The Mars atmosphere is almost made up of carbon dioxide whose dissociation energy is even lower than that of oxygen; the dissociation energy of carbon dioxide is 9.9 MJ/kg, that of oxygen is 15.5 MJ/kg. Therefore, even though the Mars entry is less energized than the Earth re-entry (for example, the flow energy, at the altitude of 90 km of the orbital entry, is about 10.9 MJ/kg for Mars and about 29.8 MJ/kg for Earth), it has to be expected that the chemical effects on the aerodynamic quantities both in the shock layer and on the surface of a space vehicle are different from those in Earth re-entry. The simulations were carried out on an axial-symmetric body, representing the nose or the first part of the fuselage of a probable aero-space-plane. The heat flux on the nose was compared considering the surface non catalytic and fully catalytic and the gas reactive and non reactive. Computer tests were made in the altitude interval 60-90 km, considering the US Standard Atmosphere 1976 model for Earth and the NASA Glenn Research Center (1996) model for Mars.

2) the second paper (2018b) was to quantify the effects of SWBLI and of SWSWI at the conditions of Mars entry and compare these effects with those at the conditions of Earth re-entry. SWBLI was studied considering an external, oblique shock wave impinging onto a flat plate on which gas was flowing and therefore a boundary layer was present. SWSWI was studied considering the interaction of the shock wave on the leading edge of an airfoil (NACA 0010) with the shock wave stemming from the airfoil concave, lower surface at the hinge position in flapped configuration. Computer tests were carried out at the altitude of 65 km, in the range of angles of attack 0-40 deg and considering three flap deflections: 0, 15, 30 deg.

3) the third paper (2019a) was to compare the effects of two Mars atmosphere models NASA Glenn and Mars Global Reference Atmospheric Model 2001 (GRAM-2001, Justus and Johnson 2001) on aerodynamics of the Pathfinder capsule along the entry path and to verify the feasibility of evaluating experimentally the ambient density by means of the method by McLaughlin *et al.* (2011) and the ambient pressure by means of the method by Cassanto (1973), therefore to reconstruct the values provided by the models. The models show consistent differences at altitudes higher than 40 km, thus the study was carried out in the altitude interval 50-100 km. Zuppardi verified that the choice of the atmosphere model is critical from an aerodynamic point of view. In fact, even starting the entry path with the same velocity due to very different values of temperature and density, the models generate completely different aerodynamic conditions. More specifically, the NASA Glenn model generates Mach and Reynolds numbers much higher and Knudsen number lower than those generated by the GRAM-2001 model.

4) the fourth paper (2019b) was to evaluate the influence of the models on 3-D Aerodynamics of Mars Pathfinder. Particular attention was paid to longitudinal moment. Computations were carried out at the altitudes of 60, 80 and 100 km, in the interval of angles of attack 0-180 deg. The study was carried out both in terms of aerodynamic force and moment and in terms of the related

coefficients. The results, in terms of dimensional quantities, were in line with dynamic pressure. The difference in the atmosphere parameters (temperature and density) between the two models generated meaningful differences in the Mach, Reynolds and Knudsen numbers which, in turn, generated changes in the profiles of the aerodynamic coefficients.

It is well known that the success of landing on a planet, provided with atmosphere, relies also on the knowledge of the atmosphere parameters. Knowledge of these parameters, with particular regard to density, strongly influences the landing procedure and its technology. For example, the low value of density of the Mars atmosphere makes inefficient the use of parachutes thus, in order to mitigate the impact of the capsule with the soil, the airbag technology was developed and implemented on the Pathfinder capsule. The subject "aerodynamics in Mars atmosphere" is topical and today gains even more importance because, as well known, the next frontier of the space exploration is the man's journey to Mars and its colonization. On the other hand, the study of this subject is not recent; it started longer than 40 years ago with the Viking I and II missions and is still today in progress, as verified by the large number of papers on several topics, ranging from theory to experiments, from Computational Fluid Dynamics (CFD) to the Direct Simulation Monte Carlo (DSMC) method. Here, for example, only a small number of recent papers are referenced:

1) Golomazov and Finkenko (2014) considered the mathematical support for the calculation of both aerodynamics and entry trajectory of descent vehicles to deliver a payload to the Mars surface. In order to determine an adequate composition of the gas, Golomazov and Finkenko studied also the dissociation reaction of carbon dioxide. Also Viviani and Pezzella (2013) evaluated the effects of chemical reactions over aerodynamics of a Mars aero-space-plane by means of a 3-D CFD code.

2) Anyoji *et al.* (2017) and Jiang *et al.* (2018) made tests in wind tunnels besides CFD computations. Edquist *et al.* (2014) analyzed aero-thermo-dynamics of the Mars Science Laboratory heat shield to withstand a fully turbulent heat pulse. More specifically, Edquist analyzed the laminar/turbulent boundary layer transition both by experimental tests, made in hypersonic wind tunnels, and by CFD computations, using a pre-flight design trajectory.

3) Raju (2015) carried out CFD computations for evaluating the aerodynamic characteristics of the Phoenix capsule at zero angle of attack. Dyakorov *et al.* (2012) analyzed the continuum static aerodynamics of the entry vehicle of the Mars Science Laboratory, including considerations for the high angle of attack of the entry vehicle, turbulent boundary layer and ablation of heat shield and other aspect relevant to the flight performance. Prabhu and Saunders (2012) evaluated by a CFD code the effects of the heat shield shape on turbulent heat flux.

4) Fei *et al.* (2016) analyzed, by means of a DSMC code, the impact of the uncertainties of the Mars atmosphere parameters on hypersonic, rarefied aerodynamics of entry vehicles.

The purpose of the present paper is to provide a contribution to the knowledge of hypersonic flow fields in Mars atmosphere. More specifically, the present paper will quantify the incidence of the above mentioned Mars atmosphere models on the chemical reactions, therefore on the aerodynamic parameters in the shock layer. Important issues in aerodynamics of a satellite or an entry body are the gas-surface interaction and the catalyticity of the body surface; these issues influence aerodynamic force and heat flux, respectively. The gas-surface interaction in low Earth orbit re-entry has been widely studied (Moe and Moe 2010 and a number of referenced papers). Atomic oxygen is absorbed by the surface of a low Earth orbit satellite or of a re-entry capsule and causes the incident air molecules to be re-emitted by a diffusive, fully accommodated model. Even though the presence of atomic oxygen is negligible in the Mars atmosphere, the gas-surface interaction has been considered diffusive fully accommodate both in the previous papers and in the

present paper.

Once again, the flow field simulations are carried out by the 2-D axial-symmetric DSMC code DS2V-4.5 64 bits (Bird 2012), simulating the Mars entry of the Pathfinder capsule in the altitude interval 50-100 km and using the two above mentioned Mars atmosphere models NASA Glenn and GRAM-2001, thus the computations are made at the same free stream conditions like those already used by Zuppardi (2019a, b).

2. Mars atmosphere models

Neither the NASA Glenn model nor the GRAM-2001 model provide information about the atmosphere composition. As reported by Williams (2016), the Mars atmosphere is made up of 7 species and its composition is constant with altitude. Table 1 reports both the mass and the molar fractions of each chemical species. Due to dissociation along an entry path, atomic oxygen and nitrogen are also present thus the Mars atmosphere is a mixture of 9 chemical species. For the purpose of the present paper, the chemical model of the Mars atmosphere, used by Bird (2005b) in the previous version 3.3 of the DS2V code, has been implemented in the current version of the code. This chemical model relies on 54 reactions: 40 dissociations, 7 forward (or endothermic) exchanges, 7 reverse (or exothermic) exchanges.

According to the NASA Glenn model, temperature (T) decreases linearly with altitude (h). The model divides the atmosphere in two zones: a lower zone up to h=7000 m, an upper zone at higher altitudes:

$$h \leq 7000 \text{ m: } T = -31 - 0.000998\, h \tag{1a}$$

$$h > 7000 \text{ m: } T = -23.4 - 0.00222\, h \tag{1b}$$

Pressure (p) decreases exponentially with altitude:

$$p = 0.699 \exp(-0.00009\, h) \tag{1c}$$

being: temperature in Celsius degrees, pressure in kilo-Pascal and altitude in meters. Density (ρ [kg/m^3]) is computed by the equation of state:

$$\rho = p / [0.1921\, (T + 273.1)] \tag{1d}$$

The GRAM-2001 model is based on the NASA Ames Mars General Circulation Model in the interval 0-80 km and on the Mars Thermosphere General Circulation Model at altitudes above 80

Table 1 Chemical composition of the Mars atmosphere

Chemical species	Mass fraction	Molar fraction
O_2	0.0013	0.00176
N_2	0.0270	0.04173
NO	0.0001	0.00014
CO	0.0007	0.00108
CO_2	0.9500	0.93399
C	0.0049	0.00396
Ar	0.0160	0.01734

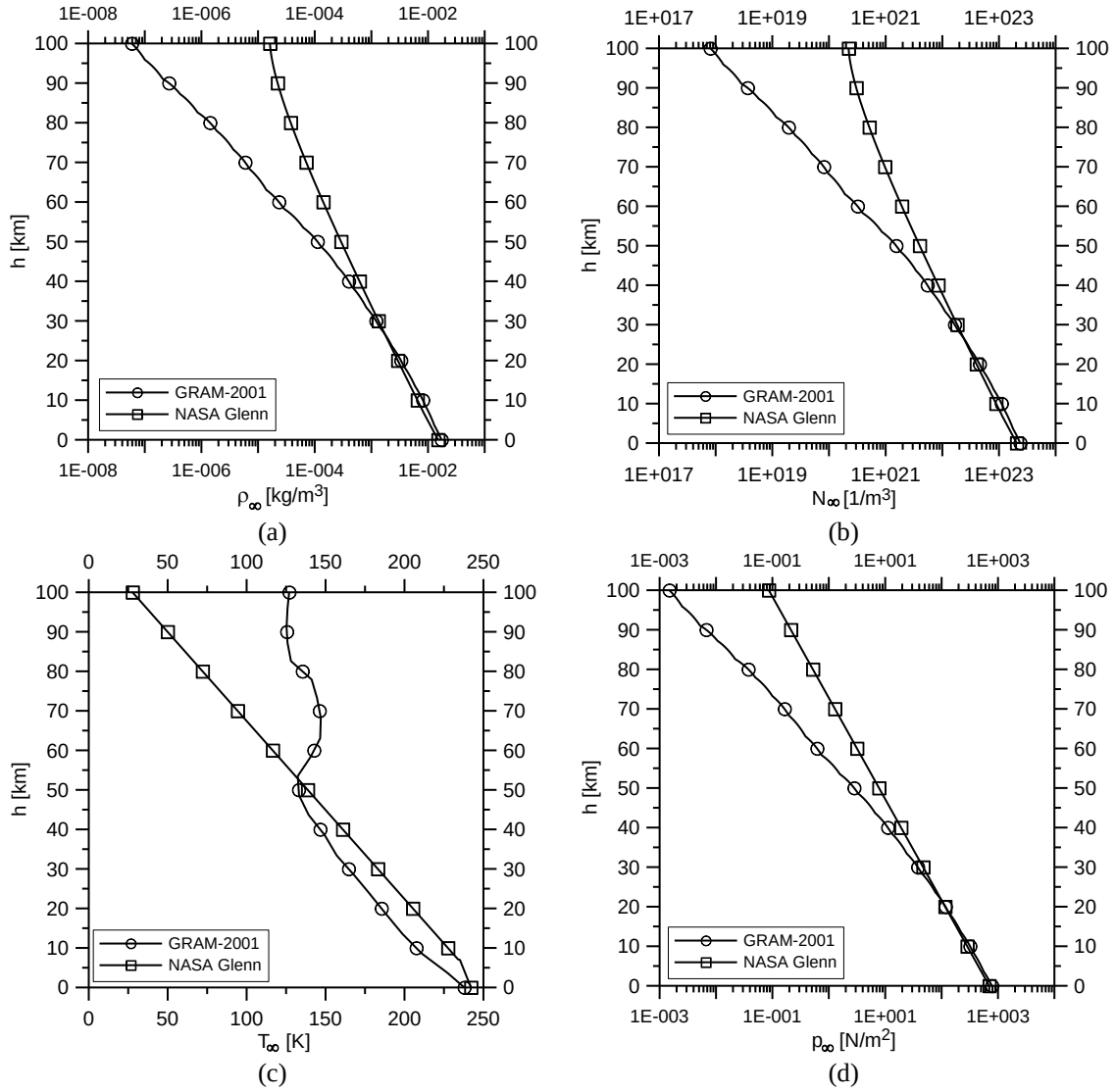

Fig. 1 Profiles of density (a), number density (b), temperature (c) and pressure (d) as functions of altitude from the Mars atmosphere models

km. Data used in the present computations (temperature, pressure and density) are those computed and reported by Justus and Johnson (2001). Output is provided as a function of altitude in the interval -1.365÷194.654 km with a step of about 5 km. For the present computations, the parameters at the intermediate altitudes in each step are computed by a linear interpolation.

Since in aerodynamic applications the ambient quantities have to be understood as free flow parameters they are labeled with the subscript ∞. Figs. 1(a)-1(d) show the profiles of density (a), number density (b), temperature (c) and pressure (d) from the two models as functions of altitude. The two models are almost equivalent in the altitude interval 0-40 km. Above 40 km, the differences increase with altitude. The most considerable difference is in temperature,

correspondingly, in density and in number density (N_∞ [1/m^3]). For example, at h=100 km, temperature is 28 and 127 K, density is 1.62×10^{-5} and 5.88×10^{-8} kg/m^3, the number density is 2.22×10^{20} and 8.05×10^{17} for the NASA Glenn and the GRAM-2001 model, respectively.

3. Mars Pathfinder entry trajectory

Mars Pathfinder is an American capsule launched by NASA on December 4, 1996 and landed on Mars on July 4, 1997. Pathfinder carried to Mars a base station with a lightweight (10.6 kg), wheeled robotic Mars rover. The rover conducted a number of experiments on the Mars surface and analyzed the composition of the soil and the morphology of the rocks. Pathfinder carried also scientific instruments and probes for sounding the Mars atmosphere.

Pathfinder is a revolution body whose geometry, in the meridian plane (x, y), is shown in Fig. 2. The curvature radius of the nose, i.e., the curve between points F and E, is 0.664 m. The curvature radius of the rounded shoulder, i.e., the curve between points D and C, is 0.0662 m and the center of curvature is located at x=0.499 m, y=1.206 m. Diameter and surface of the base area are D=2.65 m and S=5.52 m^2, respectively. The heat shield is a 70 deg cone. Pathfinder was provided of a parachute whose opening altitude was 9.4 km. Table 2 summarizes some operative parameters (Braun and Manning 2006) necessary for the present computations.

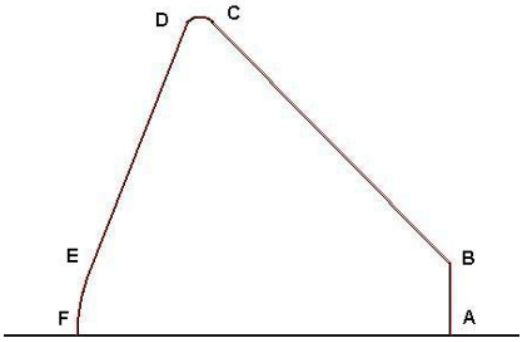

A	1.506	0.0
B	1.506	0.286
C	0.553	1.253
D	0.444	1.253
E	0.039	0.225
F	0.0	0.0

Fig. 2 Geometrical characteristics of the Pathfinder in the meridian plane (x, y)

Table 2 Pathfinder operative parameters

Type of entry	Direct
Entry velocity	7260 m/s
Entry Path Angle	14.06 deg
Entry mass	585 kg
Touchdown mass	360 kg
Entry ballistic parameter	106 [kg/m^2]
Touchdown ballistic parameter	65 [kg/m^2]
Entry angle of attack	0 deg

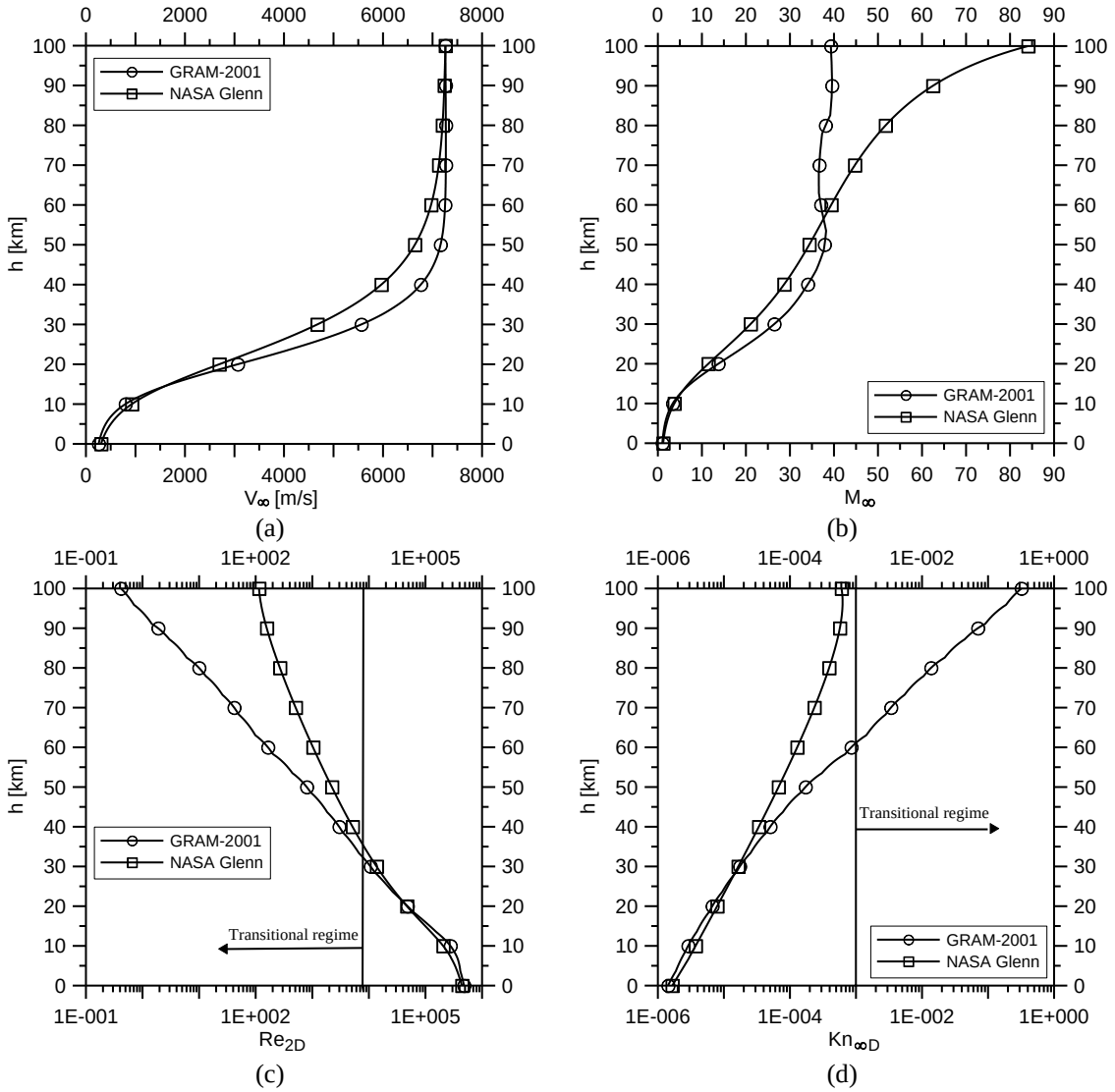

Fig. 3 Profiles of free stream velocity (a), free stream Mach number (b), Reynolds number downstream a normal shock wave (c), free stream Knudsen number (d) along the Mars atmosphere entry trajectories

The Pathfinder entry trajectory has been computed by integration of the equations of dynamics of the capsule, already used by Zuppardi and Savino (2015), considering the capsule at zero angle of attack therefore with no lift and in free entry, i.e., with no thrusters and with no parachute:

$$\frac{dV}{dh} = \frac{1}{2}\frac{\rho V}{\sin\gamma}\frac{SC_D}{m} - \frac{g}{V} \tag{2a}$$

$$\frac{d\gamma}{dh} = \frac{1}{R\sin\gamma} - \frac{g}{V^2}\frac{1}{tg\gamma} \tag{2b}$$

being: γ the flight path angle, g the gravity acceleration, R the curvature radius of the trajectory, m the capsule mass. Ratio $m/S/C_D$ is the ballistic parameter. The equations have been integrated numerically by a forward scheme with a first order approximation (Euler method), starting from h=100 km with a step of 0.1 km. For a preliminary evaluation of the trajectories, the aerodynamic drag coefficient has been assumed constant and equal to unity (C_D=1).

As reported in Table 2, due to the heat shield ablation, the Pathfinder mass reduces from 585 kg to 360 kg along the entry trajectory. Since the mass variation law along the trajectory is not known, the calculations of the trajectories have been done at the extreme conditions of m=585 kg and m=360 kg. The computations verified that at altitudes higher than 50 km, i.e., at altitudes of interest for this paper, the effects of the mass variation is negligible therefore the results shown here are those computed with m=585 kg.

Figs. 3(a) to 3(d) show the profiles of: free stream velocity, free stream Mach number, Reynolds number downstream a normal shock wave ($Re_{2D}=\rho_\infty V_\infty D/\mu_2$), free stream Knudsen number ($Kn_{\infty D}=\lambda_\infty/D$). The very low values of temperature from the NASA Glenn model produce very high values of the Mach number. For example, at h=100 km, M_∞=84 while the Mach number by the GRAM-2001 model is 39. According to: i) Vallerani (1973), the transitional regime for a blunt body is defined, in terms of the Reynolds number downstream a normal shock wave, by $10^{-1}<Re_{2D}<10^4$, ii) Moss (1995) in terms of the global Knudsen number by $10^{-3}<Kn_{\infty D}<50$. In the altitude interval 50-100 km and by both models, Pathfinder can be reasonably considered in continuum low density regime.

4. Direct simulation Monte Carlo method and DS2V-4.5 64 bits code

The Direct Simulation Monte Carlo (DSMC) method (Bird 1998, 2013, Shen 2005) is a statistical and stochastic method, solving flow fields in transitional regime i.e. from the continuum low-density regime to the free molecule regime. DSMC relies on the kinetic theory of gases and considers the gas as made up of millions of simulated molecules, each one representing a large number of real molecules in the physical space (in the present computations between 10^9 and 10^{11}).

The evolution of the molecules, in terms of velocity, spatial coordinates and internal thermodynamic/chemical status, is produced by intermolecular collisions and molecule-surface interactions within the simulated physical space. This is divided into cells both for selecting the colliding molecules and for sampling the thermo-fluid-dynamic quantities. The molecules in a cell represent those at the same location in the physical field. The method does not rely on integration of differential equation therefore it does not suffer from numerical instabilities but it is inherently unsteady with a steady solution achievable after a sufficiently long simulation time.

The basic assumption of the method is the temporal decoupling of motion and collision of the simulated molecules. The motion and collision phases are computed by two distinct algorithms, performed sequentially. This assumption holds when the evolution time step of the aerodynamic system (or global time step), is shorter than the collision time or the time between two subsequent molecular collisions. In the motion phase, the simulated molecules move ballistically at their own velocity over the global time step. Molecules change position in the flow field and interact with the surface of the body under study. In the collision phase, a couple of colliding molecules are selected in the cell. The chemical reactions take place, both colliding molecules exchange energy among the translational and the interior degrees of freedom (rotation, vibration) and change velocity. The macroscopic gas properties (density, temperature, etc.) and the macroscopic surface

properties (pressure, shear stress, heat flux, etc.) are computed by sampling and then by averaging in each cell and on each surface elemental area, respectively, molecular quantities (number density, gas composition, momentum, kinetic energy, internal energy, etc.) over a pre-fixed number (say 20÷30) of global time steps.

The DSMC code, used in the present study, is the general 2D/axisymmetric code DS2V-4.5 64 bits (Bird 2012). DS2V-4.5 64 bits is "sophisticated"; in literature, a sophisticated code is labeled also as DSMC07. A DSMC07 code implements computing procedures achieving both greater efficiency and accuracy with respect to a "basic" DSMC code; in literature, a basic code is labeled also as DSMC94. More specifically, a DSMC07 code (Bird 2006, Bird *et al.* 2009, Gallis *et al.* 2009):

1) divides the computing volume into two grids of cells (collision and sampling) with the related cell adaptation. The DS2V-4.5 64 bits code automatically generates the number of cells and the structure of the collision and sampling grids on the basis of the input megabytes (1300 in the present computations) and of the free stream number density. However, the user can change the number of cells and therefore the structure of both grids by inputting the number of molecules for the adaptation of the collision and of the sampling cells; the lower the input number of molecules per cell, the higher the number of cells after the adaptation process,

2) implements the "nearest neighbor" procedure for the selection of the potential collision partner in the collision cell. This procedure is aimed at fulfilling the physical condition that a molecule collides with the molecule closest to it. This implies that, when a molecule is chosen at random in the collision cell, the potential collision partner is the molecule closest to it. In a DSMC94 code, the potential collision partner was chosen at random from everywhere within the cell,

3) provides an optimal global time step. This is computed as a fraction (say 0.2) of the current, collision time, averaged over the computing dominion. In a DSMC94 code, the global time step was an input datum, kept constant during the evolution of the system, therefore irrespective of the actual evolving fluid-dynamic conditions,

4) avoids sequential collisions between the same collision pair. This procedure does not allow a second collision between the same collision partners; this is, in fact, physically impossible because after a collision, the molecules move away in opposite directions,

5) allows the user to evaluate the quality of a computation by means of the evaluation of the adequacy of numbers of simulated molecules and of collision cells. The ratio between the molecule mean collision separation (mcs) and the local mean free path (λ), in each collision cell, is the parameter making possible this evaluation; mcs/λ has to be less than unity everywhere in the computing domain for a good quality of a DSMC computation. Bird (2006) suggests that mcs/λ should be less than 0.2 for an optimal quality of the computation.

6) allows the user to specify the surface of the body: i) at a temperature input to each surface elemental area, ii) as adiabatic with zero heat transfer and infinite thermal conductivity, iii) as insulated with zero thermal conductivity. The thermal radiation from the surface can be also taken into account and the surface emissivity has to be input for each elemental area. In the cases of adiabatic and insulated surface, the incident heat transfer to the surface is calculated on a progressive basis and the surface temperature is adjusted such that there is no heat transfer to the surface. In the case of adiabatic surface, the code outputs a single value of temperature along the whole surface, in the case of insulated surface, the code outputs a temperature distribution on the surface.

7) provides indication about the stabilization of the DSMC computation. This is achieved when

the profile of the number of the simulated molecules, as a function of the simulated time, becomes jagged and included within a band which defines the standard deviation of the number of simulated molecules.

5. Test conditions, computation parameters and quality of the results

The analysis relies on 88 DSMC computations. In fact, for both atmosphere models and 11 altitudes between 50 and 100 km with a spacing of 5 km, the following four cases have been considered:

Case 1 non-catalytic surface, surface temperature (T_w=300 K) constant along the capsule, gas reactive,

Case 2 non-catalytic surface, surface temperature (T_w=300 K) constant along the capsule, gas non reactive,

Case 3 non-catalytic and insulated surface, gas reactive. The realistic value of 0.8, constant along the capsule, has been used for emissivity,

Case 4 fully-catalytic surface, surface temperature (T_w=300 K) constant along the capsule, gas reactive.

The results from Case 1 have to be considered as basic or reference data. Therefore, the effects of chemistry are evaluated by the comparison of the results from Cases 1 and 2. The effects of the surface temperature on pressure, skin friction and drag are evaluated by the comparison of the results from Cases 1 and 3. Similarly, the thermal analysis, in terms of heat flux, relies on the comparison of the results from Cases 1 and 4.

Table 3 reports for both models and for each altitude the input data to DS2V-4.5 64 bits: free stream velocity (V_∞), number density (N_∞), temperature (T_∞). Table 4 reports the free stream dynamic pressure ($\rho_\infty V_\infty^2$) and the energy flux ($\rho_\infty V_\infty^3$). These quantities are important because closely linked to aerodynamic force and heat flow, respectively.

Table 3 DS2V-4.5 64 bits input data from the NASA Glenn and the GRAM 2001 model

	NASA Glenn			GRAM-2001		
h [km]	V_∞ [m/s]	N_∞ [1/m^3]	T_∞ [K]	V_∞ [m/s]	N_∞ [1/m^3]	T_∞ [K]
100	7260	2.22×10^{20}	28	7260	8.05×10^{17}	127
95	7250	2.48×10^{20}	39	7262	1.64×10^{18}	126
90	7238	3.03×10^{20}	50	7265	3.66×10^{18}	125
85	7222	3.88×10^{20}	61	7267	8.61×10^{18}	127
80	7200	5.15×10^{20}	72	7269	1.94×10^{19}	135
75	7169	7.01×10^{20}	83	7269	4.08×10^{19}	143
70	7125	9.69×10^{20}	94	7268	8.09×10^{19}	146
65	7062	1.36×10^{21}	105	7264	1.56×10^{20}	147
60	6969	1.93×10^{21}	117	7253	3.20×10^{20}	143
55	6836	2.76×10^{21}	128	7226	7.13×10^{20}	135
50	6642	3.99×10^{21}	139	7161	1.53×10^{21}	133

Table 4 Free stream dynamic pressure and energy flux from the NASA Glenn and the GRAM 2001 model

	NASA Glenn		GRAM-2001	
h [km]	$\rho_\infty V_\infty^2$ [N/m^2]	$\rho_\infty V_\infty^3$ [kW/m^2]	$\rho_\infty V_\infty^2$ [N/m^2]	$\rho_\infty V_\infty^3$ [kW/m^2]
100	854	6203	3.10	23
95	954	6918	6.32	46
90	1160	8394	14.1	102
85	1481	10698	33.2	241
80	1953	14066	74.8	544
75	2632	18871	158	1145
70	3597	25632	313	2272
65	4958	35009	602	4370
60	6852	47755	1229	8917
55	9439	64519	2721	19663
50	12857	85394	5738	41091

Table 5 Computation parameters averaged over the altitude range 50-100 km: Case 1

Model	$\overline{N}_m$	$\overline{F}_N$	$\overline{N}_C$	$\overline{N}_S$
GRAM-2001	3.32×10^{7}	7.99×10^{10}	1.79×10^{6}	8.83×10^{4}
NASA Glenn	3.56×10^{7}	2.70×10^{11}	1.93×10^{6}	9.04×10^{4}

Table 6(a) Quality of results parameters: NASA Glenn model

	Case 1		Case 2		Case 3		Case 4	
h[km]	mcs/λ	t_s/t_f	mcs/λ	t_s/t_f	mcs/λ	t_s/t_f	mcs/λ	t_s/t_f
100	0.08	5.54	0.07	4.64	0.08	2.76	0.09	5.42
95	0.09	5.28	0.07	4.48	0.09	2.70	0.10	5.13
90	0.12	5.46	0.09	5.25	0.11	4.29	0.13	4.62
85	0.15	4.82	0.12	4.76	0.14	3.89	0.16	4.16
80	0.20	4.16	0.15	4.23	0.19	3.44	0.22	3.63
75	0.27	4.69	0.20	4.23	0.25	3.57	0.28	4.02
70	0.38	3.82	0.28	3.49	0.35	2.97	0.39	3.29
65	0.55	3.16	0.40	3.02	0.49	2.50	0.56	2.70
60	0.70	3.59	0.58	2.83	0.62	2.37	0.69	2.11
55	1.03	2.12	0.86	2.29	0.81	1.94	1.01	1.71
50	1.56	2.20	1.27	1.84	1.29	1.58	1.47	1.59

Table 6(b) Quality of results parameters: GRAM-2001 model

	Case 1		Case 2		Case 3		Case 4	
h [km]	mcs/λ	t_s/t_f	mcs/λ	t_s/t_f	mcs/λ	t_s/t_f	mcs/λ	t_s/t_f
100	0.0004	10.9	0.0004	9.14	0.0003	9.34	0.0004	6.62

Table 6(b) Continued

	Case 1		Case 2		Case 3		Case 4	
h [km]	mcs/λ	t_s/t_f	mcs/λ	t_s/t_f	mcs/λ	t_s/t_f	mcs/λ	t_s/t_f
95	0.0008	10.4	0.0004	9.45	0.0006	9.18	0.0009	6.89
90	0.002	15.0	0.002	8.97	0.001	8.12	0.002	10.0
85	0.001	12.9	0.003	9.16	0.003	7.79	0.004	9.43
80	0.007	11.8	0.006	8.57	0.006	7.06	0.008	7.97
75	0.02	10.9	0.01	14.9	0.01	8.96	0.02	8.07
70	0.03	8.20	0.03	12.3	0.03	6.78	0.03	6.79
65	0.06	6.10	0.05	9.44	0.05	5.07	0.06	5.13
60	0.12	6.66	0.09	6.35	0.11	4.69	0.12	5.56
55	0.28	4.23	0.19	4.36	0.24	2.91	0.28	3.57
50	0.64	2.70	0.43	2.83	0.54	2.57	0.63	2.31

The computation parameters, i.e., the number of: simulated molecules (N_m), real molecules represented by each simulated molecule (F_N), collision cells (N_C), sampling cells (N_S) did not change meaningfully either with the atmosphere model or with the altitude. For example, Table 5 reports, for both models, the values of the parameters averaged over the altitude range 50-100 km for Case 1.

The parameters quantifying the quality of the results, i.e., the ratios of mean collision separation on mean free path (mcs/λ) and of simulation time on the fluid-dynamic time (t_s/t_f), are reported in Tables 6(a) and 6(b) for the NASA Glenn and the GRAM-2001 model, respectively. The fluid dynamic time is calculated as the time necessary for the fluid to cross the length (L) of the body under study, in this case L = 1.506 m (see Fig.1) at the free stream velocity: $t_f = L / V_\infty$.

The quality of the results (defined by low values of mcs/λ and by high values of t_s/t_f), is better for the GRAM-2001 model. This is due to the lower values of density and therefore of the number density (see Figs.2(a) and 2(b)), compared with those by the NASA Glenn model. In fact, decreasing the free stream number density favors any DSMC calculation and improves the quality of the results. Even though the computations by the NASA Glenn model at h=50 and 55 km should not be rigorously accepted because mcs/λ is lightly higher than unity however, for the sake of completeness, the results have been included in the analysis.

6. Analysis of results

The effects of the atmosphere model over the flow field can be evaluated by the comparison of Figs. 4(a) and 4(b), showing the 2-D maps of temperature from Case 1, for example at the intermediate altitude of 75 km. The streamlines are also drawn on the same maps. The pictures clearly show that the shock wave by the GRAM-2001 model is much ticker than that by the NASA Glenn model. This is due to the much higher value of the free stream density from the NASA Glenn model ($\rho_\infty=5.12\times10^{-5}$ kg/m^3) compared with that from the GRAM-2001 model ($\rho_\infty=2.98\times10^{-6}$ kg/m^3). Correspondingly, the profiles of thermo-fluid-dynamic quantities in the shock layer along the stagnation line (abscissa x [m]) are smoother for the GRAM-2001 model, as

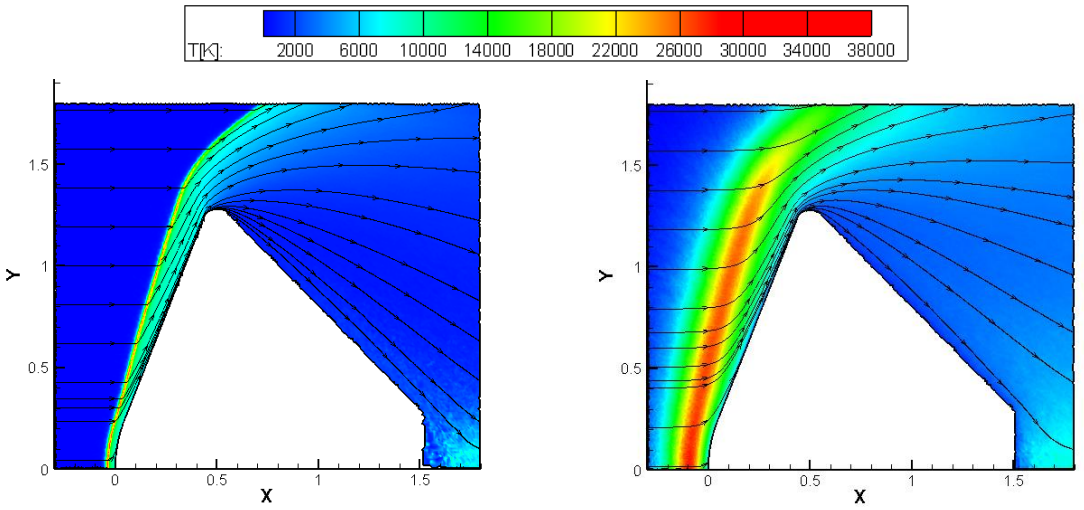

(a) (b)

Fig. 4 2-D maps of temperature and stream lines in the flow field around the Pathfinder capsule by the NASA Glenn (a) and the GRAM-2001 (b) models: Case 1, h=75 km

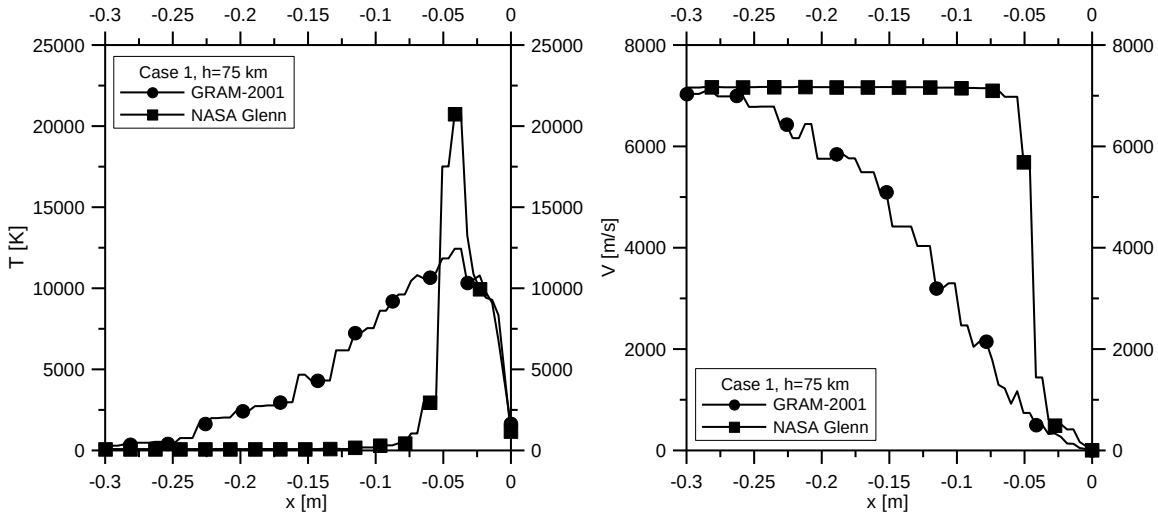

(a) (b)

Fig. 5 Profiles of temperature (a) and velocity (b) along the stagnation line of the Pathfinder capsule: Case 1, h=75 km

shown in Figs. 5(a) and 5(b) where the profiles of temperature and velocity are plotted.

The higher free stream density and energy, quantified by the total enthalpy ($H_\infty = V_\infty^2/2 + c_p T_\infty$) associated to the NASA Glenn model (Fig. 6(a)), produce an higher number (N_r) of chemical reactions (Fig. 6(b)). As expected, the profiles of N_r for both models, reproduce that of H_∞. Fig. 6(b) shows that the reactions are almost endothermic for both models.

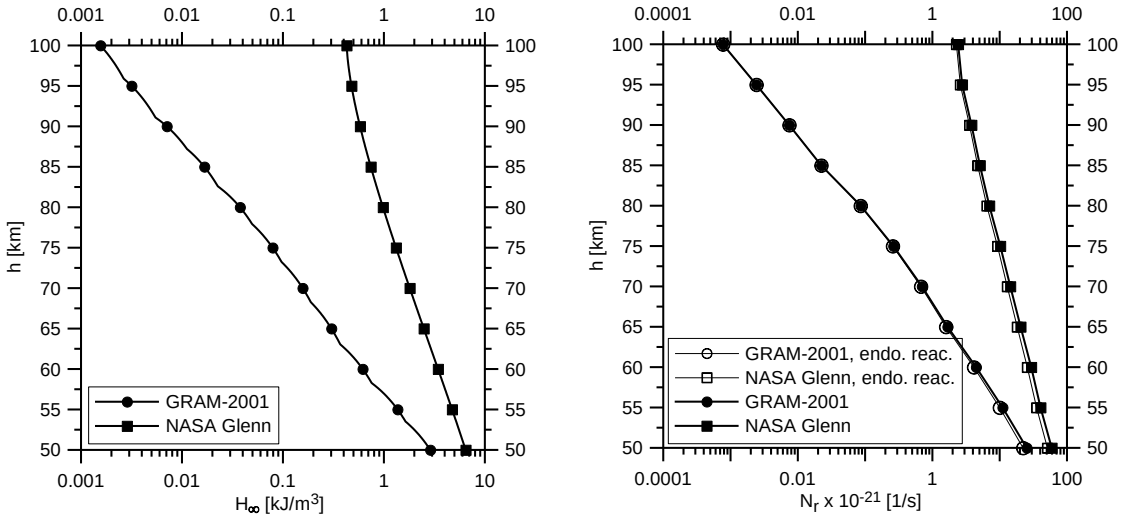

(a) (b)

Fig. 6 Profiles of the free stream total enthalpy (a) and number of reactions (b) as functions of altitude

Table 8 Average percentage variation of the shock wave intensity

	NASA Glenn	GRAM-2001
h [km]	ΔI/I%	ΔI/I%
100	41.7	44.2
95	39.1	37.5
90	46.2	48.9
85	55.2	69.7
80	41.4	33.2
75	52.9	29.8
70	29.1	40.4
65	5.4	48.8
60	76.4	39.7
55	32.4	56.3
50	87.7	37.2

The influence of the atmosphere model can be quantified also in terms of the shock wave intensity (I), here defined as the ratio of the maximum value of temperature in the shock layer and the free stream temperature ($I=T_{max}/T_\infty$). Fig. 7 shows the profiles of the intensity of the shock wave computed considering the gas as reactive (Case 1) and as not reactive (Case 2). Obviously, the absence of endothermic reactions produces values of the shock wave intensity (I) higher than those from Case 1. In order to quantify the influence of chemistry, Table 8 reports the percentage variations of the shock intensity (ΔI/I%) between Case 2 and Case 1. It seems that the influence of chemistry is equivalent for both models. In fact, the values of ΔI/I% averaged over the whole altitude interval are 46.2 for the NASA Glenn model and 44.1 for the GRAM-2001 model. The

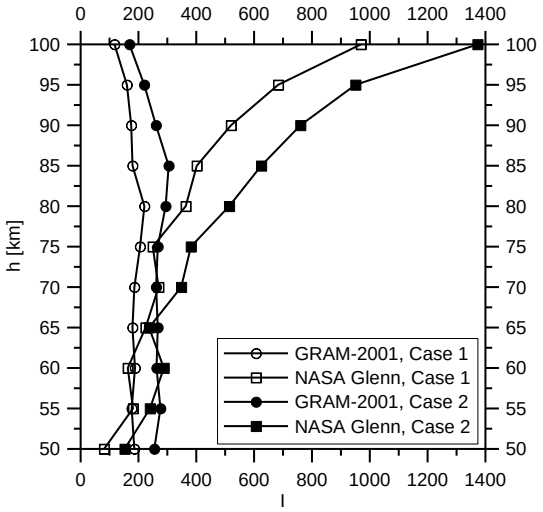

Fig. 7 Profiles of the shock wave intensity as functions of altitude

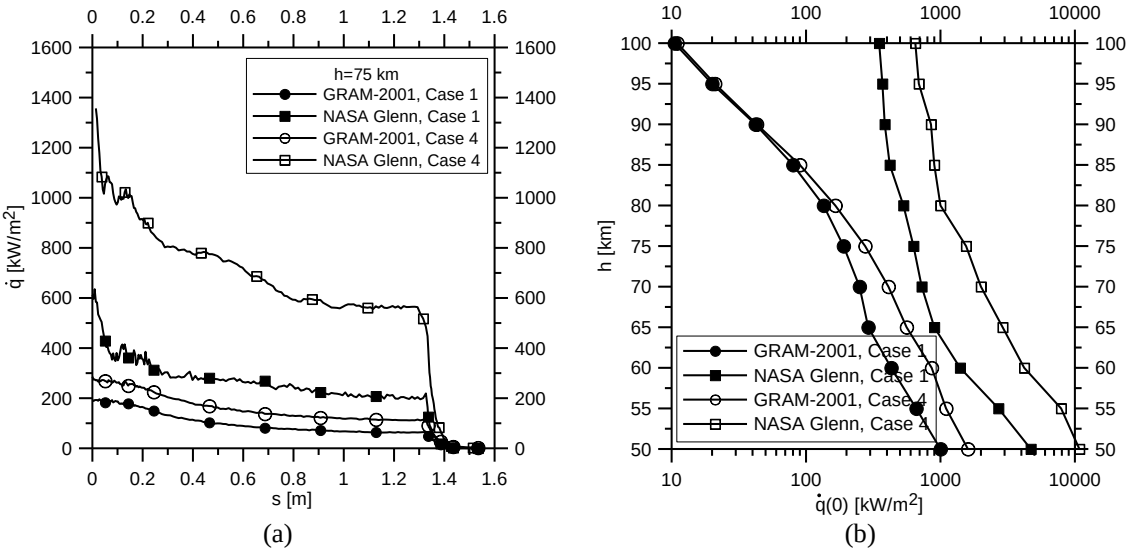

(a) (b)

Fig. 8 Profiles of heat flux along the Pathfinder surface at h=75 km (a) and heat flux at the stagnation point as function of altitude (b)

influence of chemistry can be evaluated also by means of Fig. 8(a) where the profiles of heat flux ($\dot{q}(s)$, s is the curvilinear abscissa from the stagnation point), at the intermediate altitude of 75 km along the Pathfinder surface are shown. Fig. 8(b) shows the profiles of heat flux at the Pathfinder stagnation point ($\dot{q}(0)$) as functions of altitude. The higher values of heat flux from the NASA Glenn model are due to the higher values of the free steam energy flux ($\rho_\infty V_\infty^3$, see Table 4). Furthermore, as seen before, the higher number of dissociation reactions in the flow field by the NASA Glenn model produces higher surface catalytic effects. For the GRAM-2001 model, the effects of chemistry decrease with altitude and, starting from about h=85 km, almost disappear. As

Table 9 Catalytic effects on stagnation point heat flux

	NASA Glenn	GRAM-2001
h [km]	$\Delta\dot{q}(0)/\dot{q}(0)\%$	$\Delta\dot{q}(0)/\dot{q}(0)\%$
100	85.7	4.76
95	86.5	5.00
90	121	2.38
85	114	12.5
80	88.7	22.2
75	146.	44.7
70	176	64.0
65	222	93.1
60	200	100
55	193	66.7
50	130	60.0

verified by the percentage increments of $\dot{q}(0)$ (Table 9), computed considering the surface fully catalytic and not catalytic, the catalytic effects are pretty strong for both models. Due to the higher number of dissociation reactions in the flow field, the catalytic effect is higher for the NASA Glenn model.

Fig. 9(a) shows the profiles of the insulated surface temperature along the capsule by the two models at the intermediate altitude of 75 km. Due to the higher free stream energy flux by the NASA Glenn model (see Table 4), the insulated surface temperature is higher than that from the GRAM-2001 model. For both models, the influence of surface temperature over pressure (Fig. 9(b)), skin friction (Fig. 9(c)) therefore over drag (Fig. 9(d)) is negligible. The higher values of the free stream dynamic pressure by the NASA Glenn model (see Table 4), produce higher values of the aerodynamic drag and hide the effect of the re-emission of the molecules. Table 10 reports, for both models and at each altitude, the surface temperature ($\overline{T}_W$), averaged over the whole capsule and, correspondingly, velocity ($\overline{C}_W$) and dynamic pressure ($\rho_\infty \overline{C}_w^2$) of the diffusively re-emitted molecules. The velocity of the re-emitted molecules is computed as the most probable Maxwell velocity in equilibrium at the surface temperature: $\overline{C}_w = \sqrt{2R\overline{T}_w}$, R is the gas constant. For both models, the dynamic pressure of the re-emitted molecules are two orders of magnitude lower than those of the free stream incident molecules (see Table 4).

Pressure (p(0)) and surface temperature ($T_w(0)$), at the capsule stagnation point, are important aerodynamic parameters for any entry capsule. These quantities, in fact, being the maximum values on the surface, can heavily influence the structural design of a Thermal Protection System (TPS). Figs. 10(a) and 10(b) show the profiles of p(0) and $T_W(0)$ as functions of altitude by Cases 1 and 3. The profiles of p(0) from both models agree with those of pressure along the capsule and therefore of the drag as function of altitude. Once again, due to the much higher free stream dynamic pressure and energy flux, the values of both quantities by the NASA Glenn model are consistently higher than those by the GRAM-2001 model. Table 11 reports, at each altitude, the relative differences of pressure and surface temperature of the NASA Glenn model with respect to the GRAM-2001 model.

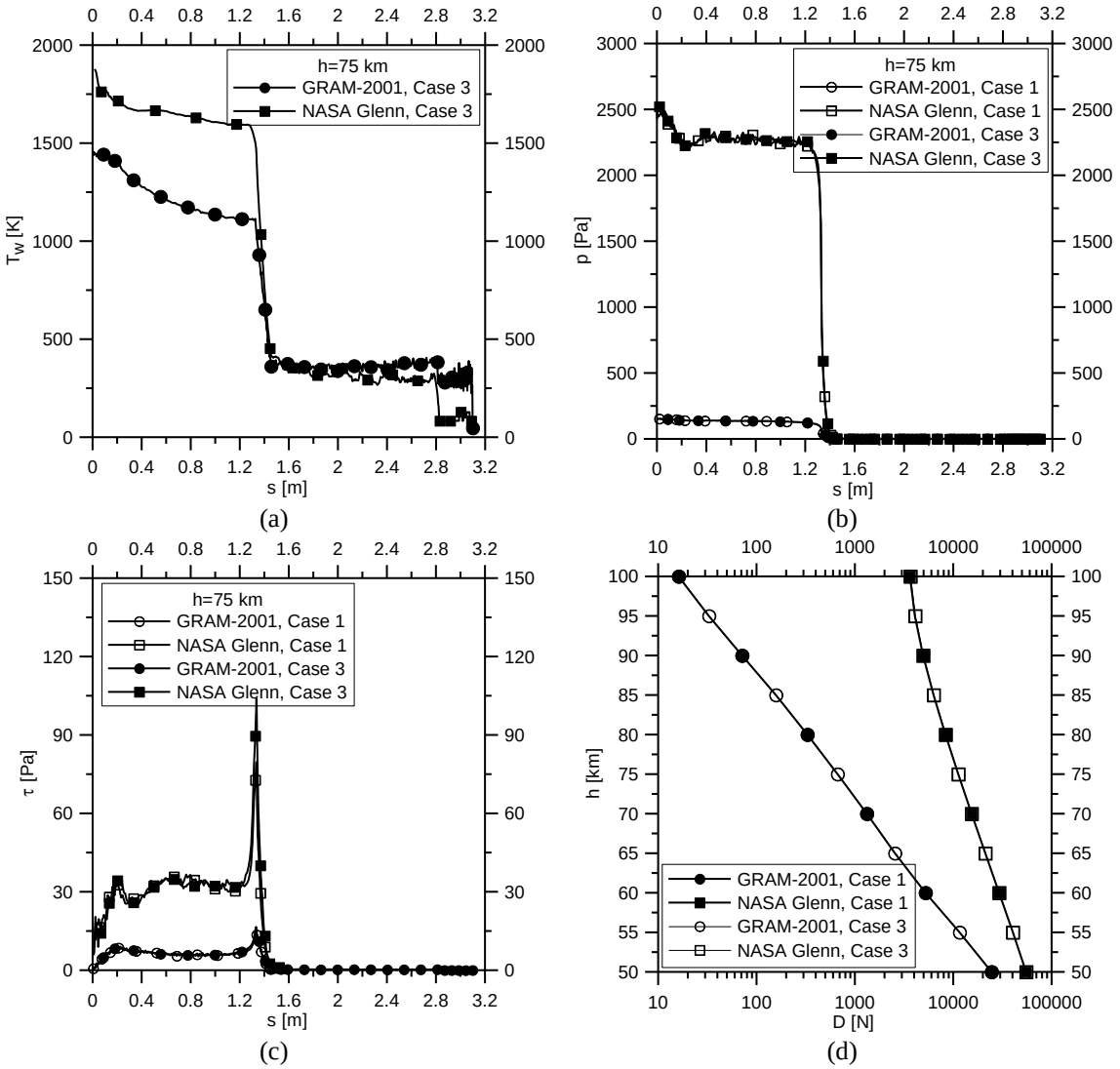

Fig. 9 Profiles of surface temperature (a), pressure (b), skin friction (c) along the capsule surface at h=75 km and drag profiles as function of altitude (d)

Table 10 Average surface temperature, average velocity and average dynamic pressure of the re-emitted molecules

	NASA Glenn			GRAM-2001		
h [km]	$\overline{T}_w$ [K]	$\overline{C}_w$ [m/s]	$\rho_\infty \overline{C}_w^2$ [N/m^2]	$\overline{T}_w$ [K]	$\overline{C}_w$ [m/s]	$\rho_\infty \overline{C}_w^2$ [N/m^2]
100	671	508	4.18	306	343	0.007
95	684	513	4.77	346	365	0.016
90	679	511	5.78	412	398	0.042
85	692	516	7.55	498	437	0.120
80	713	523	10.3	582	473	0.317

Table 10 Continued

	NASA Glenn			GRAM-2001		
h [km]	$\overline{T}_w$ [K]	$\overline{C}_w$ [m/s]	$\rho_\infty \overline{C}_w^2$ [N/m^2]	$\overline{T}_w$ [K]	$\overline{C}_w$ [m/s]	$\rho_\infty \overline{C}_w^2$ [N/m^2]
75	736	532	14.5	656	502	0.752
70	766	543	20.9	672	508	1.53
65	816	560	31.2	674	509	2.95
60	867	577	47.0	696	517	6.25
55	965	609	74.9	752	538	15.1
50	1052	636	118	837	567	36.0

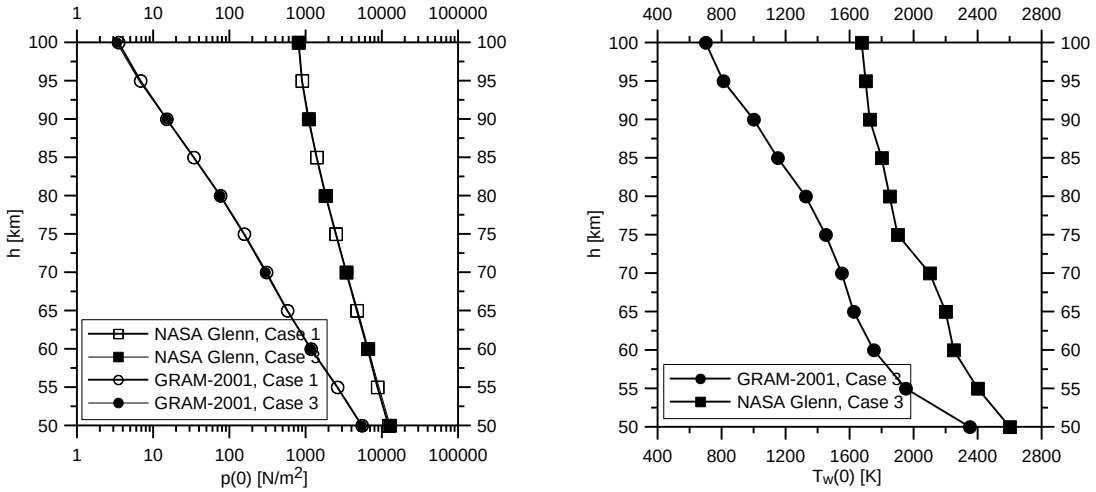

(a) (b)

Fig. 10 Profiles of pressure (a) and temperature (b) at the Pathfinder stagnation point

Table 11 Relative differences of pressure and wall temperature between the NASA Glenn and GRAM-2001 model

h [km]	$\frac{\Delta p(0)}{p(0)}$	$\frac{\Delta T_w(0)}{T_w(0)}$
100	230	1.39
95	131	1.10
90	71.5	0.73
85	40.1	0.57
80	23.2	0.40
75	14.9	0.31
70	10.2	0.35
65	7.16	0.35
60	4.55	0.29
55	2.36	0.23
50	1.24	0.11

7. Conclusions

This paper is the follow-on of four previous paper by Zuppardi on the subject "aerodynamics in Mars atmosphere". Two papers were specifically aimed at evaluating the influence of two Mars atmosphere models (NASA Glenn and GRAM-2001) over the entry trajectory and over aerodynamics of a capsule (Pathfinder). As the models show consistent difference at altitudes higher than about 40 km, the aerodynamic analysis was carried out in the altitude interval 50-100 km where the capsule was in hypersonic, rarefied flow; the solution of the flow field was carried out by means of two DSMC codes: DS2V-4.5 64 bits for the solutions of 2-D, axial-symmetric flow field, DS3V for the solution of 3-D flow fields.

With the aim of providing a further contribution to the subject "aerodynamics in Mars atmosphere" along entry path, in the present paper the effects of: i) different fluid-dynamic conditions associated to the atmosphere models, ii) chemical reactions, iii) surface temperature over local (pressure, skin friction, etc.) and global aerodynamic quantities (drag), iv) surface catalytic reactions have been quantified. The higher free stream density and flow energy, linked to the NASA Glenn model, influence both the shock wave structure and the number of chemical reactions. Apart from the catalytic effects, the results showed that the influence of the above mentioned conditions are negligible for both models and confirmed that, because of the much higher values of both dynamic pressure and energy flux by the NASA Glenn model, the effects on aerodynamics of a entry capsule are stronger than those for the GRAM-2001 model.

Certainly, the present results, as well as those already obtained by the author in previous papers on this subject, should be validated by comparison with those, either experimental or theoretical, from other researcher. Unfortunately, to the knowledge of the author, data computed at the same test conditions like those of the present and of the previous papers are not reported in literature. On the basis of the present and previous results, the opinion of the author is that the GRAM-2001 is far more reliable than the NASA Glenn model therefore the GRAM-2001 model should be always preferred to the NASA Glenn model in every space application.

References

Anyoji, M., Okamoto, M., Fujita, K., Nagai, H. and Oyama, A. (2017), "Evaluation of aerodynamic performance of Mars airplane in scientific balloon experiment", *Fluid Mech. Res. Int.*, **1**(3), 1-7.

Bird, G.A. (2005b), *Visual DSMC Program for Two-dimensional Flows*, DS2V Program User's Guide Ver. 3.3, G.A.B. Consulting Pty Ltd., Sydney, Australia.

Bird, G.A. (2005a), *Visual DSMC Program for Three-dimensional Flows*, DS3V Program User's Guide Ver. 3.3, G.A.B. Consulting Pty Ltd., Sydney, Australia.

Bird, G.A. (2006), "Sophisticated versus simple DSMC", *Proceedings of the 25th International Symposium on Rarefied Gas Dynamics*, Saint Petersburg, Russia, July.

Bird, G.A. (1998), *Molecular Gas Dynamics and Direct Simulation Monte Carlo Method*, Clarendon Press, Oxford, U.K.

Bird, G.A. (2012), *Visual DSMC Program for Two-dimensional Flows*, DS2V Program User's Guide, Ver. 4.5., G.A.B. Consulting Pty Ltd, Sydney, Australia.

Bird, G.A. (2013), *The DSMC Method, Version 1.1*, Amazon, ISBS 9781492112907, Charleston, South Carolina, U.S.A.

Bird, G.A., Gallis M.A., Torczynski, J.R. and Rader, D.J. (2009), "Accuracy and efficiency of the sophisticated direct simulation Monte Carlo algorithm for simulating non-continuum gas flows", *Phys. Fluids*, **21**(1). https://doi.org/10.1063/1.3067865.

Braun, R.D. and Manning, R.M. (2006), "Mars exploration entry, descent and landing challenges", *Proceedings of the 2006 IEEE Aerospace Conference*, Big Sky, Montana, U.S.A., March.
Cassanto, J.M. (1973), "A base pressure experiment for determining the atmospheric pressure profile of planets", *J. Spacecraft*, **10**(4), 253-261. https://doi.org/10.2514/3.61875.
Desai, P.N., Prince, J.L., Queen, E.M., Schoenenberger, M.M., Cruz, J.R. and Grover, M.R. (2008), "Entry, descent, and landing performance of the mars phoenix lander", *J. Spacecraft Rockets*. https://doi.org/10.2514/1.48239.
Desert, T., Moschetta, J.M. and Bezard, H. (2017), "Aerodynamic design of a Martian micro air vehicle", *Proceedings of the 7th European Conference for Aeronautics and Aerospace Sciences* (EUCASS-2017-365), Milan, Italy, July.
Dyakonov, A.A., Shoenenberger, M. and Van Norman, J.W. (2012), "Hypersonic and supersonic static aerodynamics of Mars science laboratory entry vehicle", *Proceedings of the 43rd AIAA Thermophysics Conference (AIAA Paper 2012-2999)*, New Orleans, U.S.A., June.
Edquist, K.T., Hollis, B.R., Johnston, C.O., Bose, D., White, T.R. and Mahzari, M. (2014), "Mars science laboratory heatshield aerothemodynamics: Design and reconstruction", *J. Spacecraft Rockets*, **51**(4), 1106-1124. https://doi.org/10.2514/1.A32749.
Fei, H., Jin, X.H., Lv, J.M. and Cheng, X.L. (2016), "Impact of Martian parameter uncertainties on entry vehicles aerodynamics for hypersonic rarefied conditions", *AIP Conf. Proc.*, https://doi.org/10.1063/1.4967684.
Gallis, M.A., Torczynski, J.R., Rader, D.J. and Bird, G.A. (2009), "Convergence behavior of a new DSMC algorithm", *J. Comput. Phys.*, **228**(12), 4532-4548. https://doi.org/10.1016/j.jcp.2009.03.021.
Golomazov, M.M. and Finchenko, V.S. (2014), "Aerodynamic design of a descent vehicle in Martian atmosphere under ExoMars project", *Solar Syst. Res.*, **48**(7), 541-548. https://doi.org/10.1134/S0038094614070089.
Jiang, H., Liu, X., Han, G. and Chen, X. (2018), "Hypersonic simulation of Mars entry atmosphere based on gun tunnel", *Proceedings of the 5th International Conference on Experimental Fluid Mechanics (ICEFM 2018)*, Munich, Germany, July.
Justus, C.G. and Johnson, D.L. (2001), *Mars Global Reference Atmospheric Model 2001 (Mars-GRAM 2001) User Guide*, NASA TM 2001-210961.
McLaughlin, C.A., Mance, S. and Lechtenberg, T. (2011), "Drag coefficient estimation in orbit determination", *J. Astronaut. Sci.*, **58**(3), 513-530. https://doi.org/10.1007/BF03321183.
Mehta, R.C. (2011), *Computations of Flow Field over Re-entry Modules at High Speed*, in *Computational Simulations and Applications*, InTech.
Moe, K. and Moe, M.M. (2010), "Gas surface interaction in low-earth orbit", *Proceedings of the 27th International Symposium on Rarefied Gas Dynamics*, Pacific Grove, California, U.S.A., July.
Moss, J.N. (1995), "Rarefied flows of planetary entry capsules", AGARD-R-808, 95-129, Special Course on "Capsule aerothermodynamics", Rhode-Saint-Genèse, Belgium.
NASA Glenn Research Center (1996), *Mars Atmosphere Model*.
Prabhu, D. and Saunders, D. (2012), "On heatshield shapes for Mars entry capsules", *Proceedings of the 50th AIAA Aerospace Science Meeting*, Nashville, Tennessee, U.S.A., January.
Raju, M. (2015), "CFD analysis of Mars phoenix capsules at Mach number 10", *J. Aeronaut. Aerosp. Eng.*, **4**(1), 1-4
Shen, C. (2005), *Rarefied Gas Dynamic: Fundamentals, Simulations and Micro Flows*, Springer-Verlag, Berlin, Germany.
Vallerani, E. (1973), "A review of supersonic sphere drag from the continuum to the free molecular flow regime", AGARD CPP 124, Paper 22, 1-15.
Viviani, A. and Pezzella, G. (2013), "Non-equilibrium computational flow field analysis for the design of Mars manned entry vehicles", *Progress Flight Phys.*, **5**, 493-516
Wei, T., Yang, X.F., Gui, Y.W. and Du, Y.X. (2015), "Aerodynamic prediction and performance analysis for Mars Science Laboratory entry vehicle", *Int. J. Aerosp. Mech. Eng.*, **9**(6), 1040-1045.
Williams, D.R. (2016), Mars Fact Sheet, https://nssdc.gsfc.nasa.gov/planetary/factsheet/marsfact.html.

Zuppardi, G. (2018a), "Effects of chemistry in Mars entry and Earth re-entry", *Adv. Aircraft Spacecraft Sci.*, **5**(5), 581-594. https://doi.org/10.12989/aas.2018.5.5.581.
Zuppardi, G. (2018b), "Effects of SWBLI and SWSWI in Mars atmosphere entry"*, Proceedings of the 31st International Symposium on Rarefied Gas Dynamics (RGD31)*, Glasgow, U.K., July.
Zuppardi, G. (2019a), "Influence of the Mars atmosphere model on aerodynamics of an entry capsule", *Adv. Aircraft Spacecraft Sci.*, **6**(3), 239-256. https://doi.org/10.12989/aas.2019.6.3.239.
Zuppardi, G. (2019b), "Influence of the Mars atmosphere model on 3-D aerodynamics of an entry capsule", *Proceedings of the Direct Simulation Monte Carlo Workshop DSMC19*, Santa Fe, New Mexico, U.S.A.
Zuppardi, G. and Savino, R. (2015), "DSMC aero-thermo-dynamic analysis of a deployable capsule for Mars atmosphere entry", *Proceedings of the Direct Simulation Monte Carlo Workshop DSMC15*, Kauai, Hawaii, U.S.A.

EC